Ocean acidification does not affect magnesium composition or dolomite formation in living crustose coralline algae, *Porolithon onkodes* in an experimental system

Nash, M.C[1] Uthicke[2], S, Negri[2], A. P., Cantin[2], N. E.*

[1]*Research School of Physics, Australian National University*

[2]*Australian Institute of Marine Science, Townsville, Queensland*

*corresponding author: merinda.nash@anu.edu.au

Abstract

There are concerns that Mg-calcite crustose coralline algae (CCA), which are key reef builders on coral reefs, will be most susceptible to increased rates of dissolution under higher pCO_2 and ocean acidification. Due to the higher solubility of Mg-calcite, it has been hypothesized that magnesium concentrations in CCA Mg-calcite will decrease as the ocean acidifies, and that this decrease will make their skeletons more chemically stable. In addition to Mg-calcite, CCA *Porolithon onkodes* the predominant encrusting species on tropical reefs, can have dolomite ($Ca_{0.5}Mg_{0.5}CO_3$) infilling cell spaces which increases their stability. However, nothing is known about how bio-mineralised dolomite formation responds to higher pCO_2. Using *P. onkodes* grown for 3 and 6 months in tank experiments, we aimed to determine 1) if mol% $MgCO_3$ in new crust and new settlement was affected by increasing CO_2 levels (365, 444, 676 and 904µatm), 2) whether bio-mineralised dolomite formed within these time frames, and 3) if so, whether this was effected by CO_2. Our results show there was no significant affect of CO_2 on mol% $MgCO_3$ in any sample set, indicating an absence of a plastic response under a wide range of experimental conditions. Dolomite within the CCA cells formed within 3 months and dolomite abundance did not vary significantly with CO_2 treatment. While evidence mounts that climate change will impact many sensitive coral and CCA species, the results from this study indicate that reef-building *P. onkodes* will continue to form stabilising dolomite infill under near-future acidification conditions, thereby retaining its higher resistance to dissolution.

1 Introduction

Determining the influence of ocean acidification from increasing CO_2 concentrations on mineral formation of crustose coralline algae is not only important to understand potential changes in CCA and their reef building capacity into the future, but also to understand the past. As atmospheric carbon dioxide (CO_2) concentrations increase, fundamental changes to the ocean's chemistry follow. Seawater pH and the carbonate saturation state (Ω) decreases, thus increasing the solubility of $CaCO_3$ skeletons. Current projections are that by the end of this century, if anthropogenic CO_2 emissions continue unabated, tropical surface seawater pH will drop by 0.3-0.4 units to ~ pH 7.8 (Orr 2011). Marine organisms forming carbonate skeletons are susceptible to increased rates of dissolution as pH declines (reviewed in Howard et al., 2012). There are concerns that Mg-calcite crustose coralline algae (CCA) will be one of the first reef-building organisms to suffer as CO_2 rises (e.g. Diaz-Pulido et al., 2012), due to the higher solubility of their skeleton. The possibility has also been raised that CCA may decrease their uptake of magnesium to form more stable lower Mg-calcite in response to higher CO_2 concentrations (e.g. Andersson et al., 2008; Ries 2011).

Experimental data on the impacts of pH on magnesium uptake by tropical CCA are limited. The branching coralline *Neogoniolithon* demonstrated a decreased magnesium concentration in experimental severely low pH conditions (Ries 2011). However, CCA *Porolithon onkodes* transplanted into low pH treatments for 8 weeks did not exhibit any magnesium composition change with pH in new surface tissue (Diaz-Pulido et al., 2014). Temperate coralline *Corallina elongate* had a variable response with new growth on existing branches not exhibiting a response to elevated CO_2 whereas new structures grown during the experiment did have decreased Mg content in higher CO_2 treatments (Egilsdottir et al., 2012). Temperate rhodoliths *Lithothamnion glaciale* did not change Mg content in different CO_2 treatments while living, however a significant decrease in the Mg content in low pH compared to dead thalli in the same treatment raised the possibility that there was a biological response (Kamenos et al., 2013). Recently it was discovered that tropical CCA *P. onkodes* commonly possess additional magnesium minerals dolomite ($Mg_{0.5}Ca_{0.5}CO_3$) and magnesite ($MgCO_3$) infilling cells in the crust

(Nash et al., 2011). This additional mineralisation significantly reduces rates of skeletal dissolution compared to *P. onkodes* without dolomite cell infill (Nash et al., 2013a). A combination of high CO_2 and increased temperature over 8 weeks led to a ~300% increase in the relative quantity of dolomite in *P. onkodes* crust transplanted into the treatment conditions (Diaz-Pulido et al., 2014). This was due to endolithic cyanobacteria, *Mastigocoleus* sp, removing calcium from the Mg-calcite skeleton but not from dolomite, leading to destruction of Mg-calcite and a relative increase in dolomite. It could not be determined if there was also an increase in the formation of primary dolomite.

When CCA grow to form the thick crust crucial to cementing together the structural reef framework, the new growth extends upwards leaving the old growth as a white crust without pink photosynthetic pigment. The pink surface of the CCA is the epithallus and the pink colouration is due to the presence of pigmented photosynthetic tissue within the Mg-calcite skeleton. In other species of corallines, this pink surface has been shown to slough off (Pueschel et al., 2005) and be grazed by chitons and limpets (Adey et al., 2013). The white crust underneath (perithallus) has been shown in other species of CCA to form as cell by cell growth downward from the meristem cells (growth layer between epithallus and perithallus) (Adey et al., 2013). Thus the white crust is a product of meristem growth, and not a build up of epithallus growth after it looses its pigmentation It is in this important reef-structure forming white crust that dolomite infill is abundant (Nash et al., 2011; Diaz-Pulido et al., 2014). As yet, there have been no experiments to determine the impact of CO_2 levels on mol% $MgCO_3$ and dolomite formation in the white crust grown in differing CO_2 treatments.

There is a noted correlation of dolomite abundance and greenhouse conditions (high temperature, high CO_2) over the geological past (e.g. MacKenzie et al., 2008; Wilkinson and Given 1986). To understand the past, it is necessary to separate the roles that CO_2 and temperature may have had on constraining dolomite concentration. This study describes the first experiments that constrain the role of CO_2 on bio-mineralised dolomite formed in differing CO_2 environments.

The aims of this investigation were threefold; 1) to identify any changes in mol% $MgCO_3$ in new settlement and new white crust of *P. onkodes* grown in Pre-industrial, Control (present day), Medium (near future) and High (end of century) CO_2 (IPCC, 2007) conditions over 3 and 6 months; 2) to determine whether bio-mineralised dolomite is formed within these timeframes; 3) to determine if the CO_2 concentration affects bio-mineralised dolomite formation.

2 Methods

2.1 Experiment

Fragments of live *P*. onkodes were collected from the upper reef crests (2 – 3 m depth) of Davies Reef (18°49.29'S, 147°37.99'E), Great Barrier Reef in August 2012. To eliminate open carbonate surfaces, CCA chips (~1 cm diameter) were sealed around the sides and base in non-toxic under water glue (Mr. Sticky's, Fair Oaks, CA) and attached to PVC slides (only the top live surfaces were exposed to seawater). Blank slides were also added to the system to identify and track new CCA settlement. Slides were mounted in custom perspex holders which were held in place on aquarium walls using magnets. The experimental system used was described in (Uthicke et al.,, 2013). Briefly, fresh filtered seawater (0.4 mm) was added to three replicate tanks (for each treatment) replacing the water twice daily. Flow rates in each experimental tank were 12 L min^{-1}. In addition to a present day (pH_T 8.0 target, measured mean 7.96 +/- 0.04 SE CO_2: 444 +/- 37 ppm), mid century 2050 (future pH_T 7.9 target, measured mean 7.90 +/- 0.04 SE CO_2: 676 +/- 37µatm) and end of century 2100 (future pH_T 7.75 target, measured mean 7.77 +/- 0.06 SE CO_2 904 +/- 32µatm) target acidification treatments, this experiment also included a pre-industrial treatment (past pH_T 8.14 target, measured mean 8.09 +/- 0.04 SE CO_2: 365 +/- 37µatm). Acidified treatments were achieved by bubbling CO_2 into sump tanks with solenoid valves (SMC pneumatics) and pH setpoints, while the pre-industrial treatment was achieved by passing a stream of air through 2 soda lime canisters and mixing the low CO_2 scrubbed air with the incoming seawater in a counter current exchange tower prior to flowing into each experimental tank. Temperatures were controlled (Avg. 26.1 ± 0.15°C) with a heater chiller unit (EvoHeat DHP40). pH and temperature were monitored continuously (30 sec sampling rate) with ISFET type pH

probes (Endress Hauser CPS-471D). Seawater CO_2 concentrations were measured using a LiCor (LI-840A) CO_2/H_2O analyser. This experiment was conducted within the outdoor aquarium facility at the Australian Institute of Marine Science under natural daily light cycles during the Austral summer (October-April). Outdoor light intensities were reduced with 70% UV blocking green shade cloth to an average intensity of 210 ± 12 µmol photons m^{-2} s^{-1}, with a daily maximum of 330 µmol photons m^{-2} s^{-1}. These light intensities correspond to the daily average light intensity on shallow reefs.

2.2 Sample selection

Subsets of CCA's in resin were removed from the tanks after 3 and 6 months. The settlement slides were removed after 6 months. Samples were randomly selected from these for XRD analyses. New crust from the resin-embedded CCA's was sampled by breaking off crust that overgrew the resin. This ensured that only crust formed during the experiment was included in the new crust analyses. The new crust typically had a thin layer (~0.5 to 2 mm) of white crust overlain by a layer of pink photosynthetic epithallus (Figure 1). CCA that had settled on the plastic slides after 6 months had only pink crust and there was no white crust underneath. Typically for the new settlement CCA, 2-4 settlement patches were required to obtain sufficient material for analysis by XRD, thus each individual result for new settlement is an average of several CCA patches. These CCA had not reached reproductive stage and could not be identified. For the 6 month experiment, CCA's in resin from the control tanks were unavailable for mineral analysis.

2.3 Analyses

CCA were cut using a bench-top saw with a 2 mm thick diamond impregnated blade. A slice through the middle of each 3-month sample was kept for SEM. Scanning Electron Microscopy-Energy Dispersive Spectroscopy (SEM-EDS) was undertaken at the Australian National University using a Ziess UltraPlus field emission scanning electron microscope (FESEM) equipped with an HKL electron backscatter diffraction (EBSD) operated at 15kV, 11 mm working distance. CCA were mounted using carbon tape and carbon coated. Subsampling for XRD was taken from the matching side of the remainder crust. Xray diffraction and mineral determination was carried out following Nash et al.,

(2013b). Simply, this method uses the asymmetry off the higher 2-theta side of the Mg-calcite XRD peak to detect dolomite. The more asymmetry the greater proportion of dolomite in the crust. A shoulder off the higher 2-theta side of the peak indicates magnesite ($MgCO_3$) is also present. This asymmetry and shoulder is captured with the asymmetry mol% measurement. The asymmetry mol% is used to compare for differences in relative dolomite and magnesite quantities (Nash et al., 2013b). It is not a measurement of absolute quantity, however when compared to mineral quantities determined using standard curve fitting techniques, the differences in asymmetry well reflect the differences in dolomite and magnesite quantities (as used in Diaz-Pulido et al., 2014). See Figure 1 (Supplement) for example scans.

2.4 Dolomite terminology

Stoichiometric dolomite is 50 mol% $MgCO_3$. Typically dolomite formed under high temperature is stoichiometric and well ordered (Kaczmarek and Sibley 2011). Ordering occurs where there are alternating layers of $MgCO_3$ and $CaCO_3$ in the calcite lattice, whereas completely disordered dolomite has Mg randomly substituting for Ca in the lattice. Sedimentary dolomite formed at sea surface temperature and pressure and not subject to post-deposition burial and metamorphism, typically is non-stoichiometric with a range of 37.5 to 52 mol% $MgCO_3$ (Jones et al., 2001) and not well ordered (Kaczmarek and Sibley 2011). Synthetically formed disordered dolomite has been shown to be unstable in aqueous solutions and therefor it is thought that disordered dolomite cannot form or persist in the open marine environment in which sedimentary dolomite forms (Gaines 1977). A variety of descriptions exist for dolomite that deviates from stoichiometric and perfectly ordered; non-ideal, poorly ordered or disordered, protodolomite, pseudo-dolomite and calcium enriched dolomite (Gaines 1977).

Here we use the term dolomite to represent magnesium calcite in the range 38-62 mol% $MgCO_3$, as measured for CCA *P. onkodes* dolomite (Nash et al., 2011) without inferring cation ordering status, that is, whether it is ordered, disordered or partially ordered. The CCA *P. onkodes* dolomite has previously been demonstrated via etching experiments and natural dissolution processes to have a delayed dissolution reaction compared to Mg-

186 calcite and has different crystal forms to Mg-calcite (Nash et al., 2013a). Furthermore, it
187 has been documented that Mg-calcite in CCA *P. onkodes* ranges up to ~26 mol% $MgCO_3$
188 (Nash et al., 2011) and there is a well-defined division from dolomite which commences
189 at ~38 mol% $MgCO_3$. Experimental work has demonstrated that cyanobacteria
190 (*Mastigocoleus* sp) which bio-erode limestone by removing calcium, do not take calcium
191 from dolomite rock (Ramirez-Reinat and Garcia-Pichel 2012). Experiments on live
192 dolomite-forming CCA *P. onkodes* also show that the same cyanobacteria remove
193 calcium from CCA Mg-calcite but do not remove calcium from the *P. onkodes* dolomite.
194 *P. onkodes* Mg-C and *P. onkodes* dolomite have distinctly different physical properties
195 and *P. onkodes* dolomite reacts under chemical (Nash et al., 2013a) and bio-erosion
196 conditions (Diaz-Pulido et al., 2014) comparably to dolomite the rock. We have been
197 unable to confirm the presence of ordering peaks by XRD for the dolomite within the
198 living *P. onkodes* (Nash et al., 2013b). However the persistence of the CCA dolomite in
199 aqueous environments and its greater resistance to dissolution than Mg-calcite (Nash et
200 al., 2013a) suggests there is some degree of ordering and CCA *P. onkodes* dolomite is not
201 the same mineral as Mg-calcite which theoretically becomes less stable with greater Mg-
202 substitution (Andersson et al., 2008). Therefore we consider that referring to the CCA
203 mineral as dolomite, with the caveat that this is without inferring cation-ordering status is
204 the most appropriate identification for the mineral at this time. Our decision to use this
205 terminology for Mg-C > 38 mol % $MgCO_3$ is supported by recently published
206 clarification on terminology for Ca-Mg carbonates (Zhang et al.,, 2015).

207

208 2.5 Crust terminology
209 The term 'pre-experimental growth' refers to crust grown in situ at Davies reef prior to
210 collection for the experiment. The new crust (experimental) is the growth above the
211 height of the resin. The 'new crust' terminology is used because this includes both the
212 white crust of the perithallus and the pink surface epithallus. There may also be
213 regrowths within the white crust that includes hypothallus cells and alteration to aragonite
214 (see for example Fig. 8). The new settlement on slides in the 6 month treatment was
215 predominantly pink indicating epithallus growth. However when CCA settle, the first

cells laid down are hypothallus cells growing lengthways parallel to the surface and then vertical growth of the epithallus, followed by the perithallus (Steneck 1986). A scraping sample would include not only epithallus but also minor hypothallus and possibly the start of a perithallus. For this reason we use the term new settlement rather than epithallus

2.5 Statistical analysis

We tested for difference between CO_2 treatments and sample type using two factor analysis of variance (ANOVA). Different CO_2 treatments (Factor Treatment) and experimental growth versus pre-experimental growth (Factor Type) were both used as fixed factors. Residual plots and boxplots confirmed that there were no deviations from ANOVA assumptions. Because slightly unequal sample sizes were used in each treatment, we applied marginal sums of squares for the F-tests.

3 Results

3.1 Mineral composition in different CO_2 treatments

We investigated the mineral composition of CCA exposed to different OA conditions for 3 and 6 months in a long-term aquarium experiment. There were no significant differences in mineral composition between any of the CO_2 treatments (Table 1). For the new *P. onkodes* crust formed during the 3 month duration (Figure 2a), the mol% $MgCO_3$ range is 16.4 – 16.7 mol% $MgCO_3$ (n = 5 per treatment, averages: Pre 16.6, Control 16.5, Medium 16.4, High 16.7 mol% $MgCO_3$) (full results supplement Table 1). This range is only 0.1 mol% more than measurement precision (Nash et al., 2011). For the new *P. onkodes* crust formed over 6 months (Fig. 2b), the mol% $MgCO_3$ range was the same as the 3 month crust 16.4 – 16.7 mol% $MgCO_3$, (Pre 16.7 n=5, Medium 16.4 n=3, High 16.5 mol% $MgCO_3$ n=6) (Supplement Table 2). Many of the Mg-calcite XRD peaks for both the 3 and 6 month crust demonstrated asymmetry indicating the presence of dolomite (as per Nash et al., 2011, 2012, 2013a,b, Diaz-Pulido et al., 2014) however there was no significant difference in the dolomite asymmetry related to CO_2 treatments (asymmetry test, Table 1). For unidentified CCA that had settled on the slides over 6 months (Fig. 2c), (Supplement Table 3) the mol% $MgCO_3$ ranged from 14.7- 14.9 (Pre 14.8 n=3, Control n=4 14.7, Medium 14.7 n=5, High 14.9 mol% $MgCO_3$ n=5). The new settlement

CCA did not have dolomite, i.e. no peak asymmetry, consistent with the absence of white crust underneath.

3.2 Mineral compositional differences between crust layers

As there was no significant difference between treatments, all treatments were combined for each time period. There was a significant difference in magnesium composition between experimental crust and pre-experimental crust. Mg-calcite mol% $MgCO_3$ was also significantly different for new settlement (pigmented growth without development of white crust) compared to new crust (growth that has developed white crust). The 6 month new settlement (pigmented growth only) at 14.8 mol% $MgCO_3$ (Fig. 3) was significantly lower than the mol% $MgCO_3$ for the new crusts from the 3 and 6 months new crusts (~16.5 mol% $MgCO_3$). The asymmetry indicating dolomite presence was absent from the new growth, but appeared in new white crust within 3 months (Asymm mol % 17.6) and was higher again for the 6 month new crust (Asymm mol % 18.7). The mol% $MgCO_3$ and asymmetry mol% in the pre-experimental *P. onkodes* crust (the crust formed in the natural environment prior to sample collection) were even higher at 17.5 and 21.6 mol% $MgCO_3$ respectively (Fig. 3) (full data Supplement Table 4).

3.3 SEM results

3.3.1 Comparison of crust across treatments and experimental / pre-experimental

Although there was no detected difference in mineral composition across treatments, SEM was undertaken to visualise potential differences in calcification structures between treatments. There was no visible difference in calcified crust detected between CCA from pre-industrial, control or high CO_2 treatments. There was however, a clear difference in the structure of the crust grown during the experimental duration compared to the pre-experimental crust (Figs. 4, 5 and supplement Fig. 2). This difference was observed in control CCA, as well as pre-industrial and high CO_2 CCA indicating the difference was not related to the CO_2 levels. Crust formed during the experiment appeared less organized and also appeared structurally less dense (Fig. 6) with cracks and associated gaps in the crust that were not present in the pre-experimental crust. The difference in density was based on observation and not able to be quantified.

The experimental crust had compressed under the action of the saw used to slice the CCA (Fig. 7). We note that this compression by the saw would have made it difficult to identify any differences in growth structure between the CO_2 treatments. Previous work relying on SEM for CCA interpretation has used both saw cutting similarly to here (Nash et al., 2011, 2013a, b; Diaz-Pulido et al., 2014) as well as fracturing without any further treatment of the sample (Nash et al 2013a, Diaz-Pulido et al., 2014). There has not been an observed impact of saw cutting on experimental samples (Diaz-Pulido et al., 2014) however those previous samples were polished after cutting and fine cracks may have been less obvious due to polishing. The crust features in the pre-experimental crust are comparable to features in other CCA *P. onkodes* analysed using SEM that have been cut, cut and polished or only fractured (Nash et al., 2011, 2013a,b; Diaz-Pulido et al., 2014) and it is unlikely that the use of the saw has introduced an artifact into this study other than to highlight the susceptibility of the experimental crust to crushing compared to pre-experimental crust.

3.3.2 Dolomite features

Dolomite composition determined by SEM-EDS ranged from 37.3 to 59.8 mol% $MgCO_3$ (Table 5 Supplement), comparable to the range identified in previous studies (Nash et al., 2011). There was a de-lineation along the new experimental growth where dolomite was nearly absent compared to consistent infill in pre-experimental crust (Figs 5-7, Supplement Fig. 3). The structure of dolomite formed in the experimental crust also appeared different to that which formed in the pre-experimental crust (Fig. 4). New growth dolomite did not generally fill the cells as was observed in the pre-experimental growth. In the experimental growth, dolomite was present as lumpy infill or lining (Fig. 4 a and b). In the pre-experimental crust, dolomite lined and in-filled most cells (Fig. 4 c and d). In the control CCA the pre-experimental crust had an opaque organic film that was not visible in experimental growth (Fig. 5c), although there was organic material in the cells (Supplement Fig. 3).

3.3.3 Crust damage possibly due to transfer to experimental tanks

Pre-experimental crust immediately below experimental growth had aragonite cell infill (Fig. 7). In previous work aragonite infill of this type has only been observed at the base of the CCA crust exposed to seawater (Nash et al., 2013a Supplement), or in parts of the skeleton that have been damaged allowing seawater to penetrate. However, we could find no obvious signs of damage to the crust. CCA *P. onkodes* has varied mineralogy throughout the pre-experimental crust (Fig. 8) with patches altered to aragonite and dolomite bands. Regrowth in damaged areas within the pre-experimental crust was more dolomite rich than surrounding areas (Fig. 8b) indicating that damage to crust in the open environment had not resulted in a reduction in dolomite formation.

4 Discussion

Our results show that over the experimental duration 1) there were no changes in any crust mineral composition relating to CO_2 concentrations; 2) bio-mineralised dolomite forms within 12 weeks within aquarium conditions; and 3) CO_2 concentrations do not affect bio-mineralised dolomite formation.

4.1 Magnesium composition and calcification processes

The higher mol%$MgCO_3$ for white crust compared to the pigmented new growth layer (new settlement) has been documented previously for *P. onkodes* (Diaz-Pulido et al.,, 2014). This higher mol%$MgCO_3$ in the white crust suggests that controls on magnesium uptake are different for the white crust (perithallium) than the pigmented surface layers (epithallium).

Considering that CCA crusts are increasingly being used for paleo environmental reconstruction (e.g. Kamenos et al., 2008; Halfar et al., 2013; Caragnano et al., 2014; Darrenougue et al., 2014; Fietzke et al., 2015), it is important to know whether this difference in magnesium composition between the pigment surface and white crust is part of the standard calcification processes of the CCA or due to post-depositional change. In this and previous work (Nash et al., 2011, 2013a) portions of the crust that have been diagenetically altered post-deposition have cells in-filled by aragonite or Mg-calcite.

Typically the cell walls have not exhibited evidence of alteration even when there has clearly been exposure to seawater suggesting the intact cell walls are quite resistant to diagenesis. Probably the epithallus cell walls and perithallus cell walls have differences in the organic material that constrains the Mg uptake. The interfilament and intrafilament (spaces between adjacent cell walls) calcification does not appear to be physically constrained by an organic template. Mg-calcite crystals are randomly orientated (Nash et al., 2013a; Adey et al., 2013) or roughly parallel to the cell walls which suggests that the controls on calcification and consequently Mg incorporation may be different again for the interfilament calcification. It seems most likely that the difference in the mol% MgCO3 for the white crust compared to the pigmented new growth is due to organism-constrained Mg uptake during the crust development. It cannot be determined from this study whether the Mg is incorporated in its final concentrations as the new cell wall and inter/intra filament calcification is first formed or if there is subsequent Mg enrichment over days/weeks/ months. However, previous work subsampling portions of the CCA crust from the top to the base has not demonstrated any systematic increase in mol% MgCO3 (Nash et al., 2013b) suggesting if there is post-deposition Mg enrichment, it occurs relatively contemporaneously with growth.

The consistency of magnesium composition across *P. onkodes* and new settlement CCA from pre-industrial to high CO_2 treatments does not provide support for the theory that Mg-C organisms will take up less magnesium under higher CO_2 conditions (Andersson et al., 2008). Instead our results agree with the response of *P. onkodes* in an 8 week laboratory aquarium experiment which also showed no change in mol% $MgCO_3$ in pigmented growth with CO_2 levels up to 1225µatm (Diaz-Pulido et al., 2014). Those CCA were not embedded in resin and were grown in higher temperatures (28 and 30 degrees). Both these aquarium experimental results are in agreement with new settlement CCA in CO_2 enriched flow through systems (Kuffner et al., 2008). This consistency of mol% $MgCO_3$ suggests there is a strong biological control on magnesium uptake under variable CO_2 concentrations and no detectable plastic response to CO_2 within the experimental ranges. The absence of change across treatments for mol% $MgCO_3$ in the

370 new settlement CCA, none of which have dolomite, suggests that the similar apparent
371 lack of response of the mol% $MgCO_3$ in the white crusts to CO_2 treatments is unrelated to
372 the presence of dolomite. The lack of difference between pre-industrial, medium and high
373 treatments in the 6 month crust sample set suggests that no trends have been missed with
374 the absence of the control group.
375
376 **4.2 Comparison to other studies**
377 The results from the *P. onkodes* are in contrast to the decreased magnesium composition
378 for tropical branching *Neogoniolithon* sp. (Ries 2011). This form of *Neogoniolithon* is
379 not abundant in the high-energy environments that *P. onkodes* dominates. However, the
380 mol% $MgCO_3$ measured in the *Neogoniolithon* control (~18.7 - 21.3 mol% $MgCO_3$) was
381 much higher and with greater range than that measured for *P. onkodes* in this experiment
382 (pre-experimental crust 17.2-17.9, 3 month crust 16-16.8, new settlement 14.4-15.3
383 mol% $MgCO_3$ Supplement tables 1, 3 and 4). The mol% $MgCO_3$ in the *Neogoniolithon*
384 decreased to 18.7-16.7 mol% at 903µatm CO_2 (equivalent CO_2 levels as our highest
385 treatment) but only decreased by another 1.3 mol% $MgCO_3$ on average (range 17.3-16.0
386 mol% $MgCO_3$) with an extra 1962 µatm (2865 µatm CO_2). Thus the lowest Mg levels
387 for the *Neogoniolithon* in the highest CO_2 treatments were comparable to our results for
388 control (and treatments) and to other *P. onkodes* collected from the Great Barrier Reef
389 (Nash et al., 2011; Diaz-Pulido et al., 2014). This raises the possibility that CCA Mg-C
390 levels are susceptible to change as CO_2 rises but only for levels higher than a stable
391 baseline, which for the tropical corallines may be in the range of ~16-17.5 mol%
392 $MgCO_3$. Egilsdottir et al., (2012) working on the temperate articulated coralline
393 *Corallina elongata* reported a significant decrease in Mg content for new structures
394 formed under CO_2 550-1000 µatm. For tips, branches and basal parts formed under the
395 enriched CO_2, Mg content ranged from 14.7 – 15.9 mol% $MgCO_3$ and was not
396 significantly different from controls (15.7, 15.2, 15.4 mol% $MgCO_3$ respectively). On
397 the other hand, structures growing off the base exhibited 16 % $MgCO_3$ under control
398 conditions but reduced in the tips, branches and basal plates of these new structures (15.1,
399 14.9, 15.3 mol% $MgCO_3$) at 550 µatm CO_2. These results suggest there is a different
400 calcification process for the new structures compared to the tips, branches and basal parts

401 and that this calcification process is sensitive to CO_2 but only up to 550 µatm. Research
402 on temperate coralline *Lithothamnion glaciale* showed no changed in [Mg] for new
403 growth over 80 days in reduced pH 7.7 treatments (Kamenos et al., 2013).
404
405 Work on CO_2 influences on coralline algae structure has to date been on temperate
406 corallines (e.g. Burdett et al., 2012; Egilsdottir et al., 2012; Ragazzola et al., 2012, 2013;
407 Hofmann et al., 2012; Kamenos et al., 2013). Experiments on living tropical CCA
408 calcification have focused on weight changes (e.g. Anthony et al., 2008; Comeau et al.,
409 2013; Johnson et al., 2014) and impacts on existing crust mineralogy (Diaz-Pulido et al.,
410 2014). There is little specific information known about calcification processes in tropical
411 crustose corallines. However as this study and previous studies on mineralogy (Nash et
412 al., 2011, 2013b; Diaz-Pulido et al., 2014) show, carbonates in CCA are not only Mg-
413 calcite but can also include dolomite, magnesite and aragonite. It is clear that the net
414 mass of CCA is a result of multiple mineral-forming processes. While all form within the
415 biological structure it seems unlikely that infill dolomite, magnesite and aragonite are all
416 the result of organism controlled calcification processes and instead are biologically
417 induced. Thus experimental net weight changes for *P. onkodes* may not always be a
418 reflection of changes for only Mg-calcite calcification and/or dissolution.
419
420 Aragonite can form as a result of parasitic endolithic bacterial activity within the CCA
421 (Diaz-Pulido et al., 2014) and contribute to measured weight gain. In the Diaz-Pulido et
422 al., study (2014) weight change was due in part to a mix of bacterial-driven carbonate
423 destruction processes and abiotic aragonite precipitation as a result of calcium
424 mobilisation by the endolithic bacteria. In the Johnson et al., (2014) study weight gain by
425 CCA from locations downstream of the reef front was interpreted as indicating
426 acclimatisation. However if there were more endolithic bacteria present in their
427 downstream CCA than the reef front CCA, it is possible that the experimental fluctuating
428 conditions with elevated CO_2 activated bacterial processes and the lower CO_2 resulted in
429 increased re-precipitation of mobilised calcium as aragonite (aragonite re-precipitation
430 transforms the porous crust to dense cement) which could account for a proportion of the
431 weight gain. Therefore it is problematic to presume acclimitisation based on weight gain

without knowing how the weight was gained. The published experiments referred to in this discussion were all conducted prior to the discovery of dolomite, magnesite and aragonite in CCA *P. onkodes*, but future studies should consider the more complex nature of mineral composition of *P. onkodes* when attempting to explain weight changes and calcification (e.g. Nash et al., 2013).

The varied responses of the tropical and temperate corallines to altered CO_2 indicate that the uptake of Mg by CCA is not consistent across all species or even within the same organism (Egilsdottir et al., 2012). Furthermore, the use of different methods of measuring magnesium concentration potentially complicates comparisons across data sets. Ries (2011) and our study used XRD to determine mol% $MgCO_3$. This measurement only returns mol% for the Mg-Calcite component and is not influenced by the presence of magnesium in other forms, e.g. dolomite or within organics, or diluted by the presence of aragonite. Kamenos et al., (2013) used Raman spectroscopy for identifying mol% $MgCO_3$ changes, this method is not widely used for coralline algae mineralogy studies. Egilsdottir et al., (2012) used inductively coupled plasma- atomic emission spectroscopy (ICP-AES) to quantify bulk magnesium and Ragazzola et al., (2013) used electron microprobe to obtain an average elemental composition for Mg/Ca ratios. These methods return bulk magnesium for the total sample or portion under the electron beam and may be skewed by undetected aragonite, common in corallines (Smith et al., 2012; Nash et al., 2013b) or presence of Mg not within the Mg-calcite, (e.g. Caragnano et al., 2014).

4.3 Dolomite formation within 12 weeks

Prior to the discovery of bio-mediated dolomite in association with bacteria (Vasconcelos and Mackenzie 1997) and CCA (Nash et al., 2011,) dolomite was thought to form by chemical alteration of limestone over geological time frames, e.g. thousands to millions of years (e.g. Saller 1984). Although it has also been controversially argued that dolomite was the primary precipitation in some ancient dolomite formations (Tucker 1982). Our experimental results demonstrate that bio-mineralised dolomite formation is rapid and occurring contemporaneously with the surrounding limestone formation. The

apparent reduction in dolomite formation in the experimental conditions compared to the pre-experimental growth indicates that there is also a rapid response to changing environmental conditions. Accordingly, any interpretation of past environments made using dolomite that may have had a biological origin, i.e. dolomite in formerly shallow tropical environments, would need to take into account this potentially rapid formation and response to environmental change.

4.4 Implications for interpreting the geological past

The absence of a significant effect of CO_2 on dolomite formation in this experiment suggests that the observed correlation in the geologic rock record of dolomite and greenhouse conditions may not be a direct result of high CO_2 driving increased primary bio-mineralised dolomite formation. However, as noted in previous work (Nash et al., 2013a; Diaz-Pulido et al., 2014) dolomite is more resistant to chemical dissolution and biological erosion than Mg-calcite (and presumably also calcite). Therefore the positive correlation of dolomite and greenhouse epochs in the rock record (e.g. MacKenzie et al., 2008; Wilkinson and Given 1986) may be due in part to preferential preservation of bio-mineralised dolomite compared to surrounding skeletal material, rather than CO_2 or temperature driven biological processes leading to increased dolomite formation. Furthermore, during greenhouse times, sea level was higher thereby providing greater area of warm shallow (epeiric) seas and thus more accommodation space for calcifying algae that may have formed dolomite. While past primary bio-mineralised dolomite levels may not have been directly linked to CO_2 levels, there is certainly support from other work (Nash et al., 2013a; Diaz-Pulido et al., 2014) for indirect biologically-associated processes leading to increased abundance of bio-mineralised dolomite under higher CO_2 conditions.

4.5 Changes in calcification in experimental tanks

Considering the aragonite observed in the crust where the CCA was transferred to the experimental tanks, it may be that interruptions to normal growth after transfer to experimental tanks, allowed seawater to penetrate into the shallow surface layer resulting in alteration of Mg-C to aragonite. Previous experiments on calcification rates of CCA

found that rates of photosynthesis, and production of inorganic and organic carbon, were significantly lower in experimental tanks than *in situ* (Chisholm, 2003). A decrease in photosynthesis and calcification rates may be the explanation for the observed differences in calcified crust in this study, although the exact mechanism leading to the change is not known. The absence of the organic film in the experimental growth (Fig. 5c) raises the possibility that it is the absence of these organics that has led to the observed differences in calcification. This organic film is consistently present on the pre-experimental growth and consistently absent from the experimental growth. Thus it is unlikely to be a sample preparation artifact, although the preparation method may make this film more readily visible than if the samples had been fractured leaving an uneven surface. Reduced organic production may also lead to less dolomite as experiments have shown that dolomite nucleates on polysaccharides produced by red algae (Zhang et al., 2012). It is probable that our experimental results understate how much dolomite could be formed in the open marine environment over a 3 and 6 month period.

The observation that the change to experimental tanks coincided with changes in CCA calcification has implications for extrapolating experimental results back to the natural environment. There is a substantial change in the ultra structure and secondary mineralisation (i.e. formation of dolomite) processes. While comparisons between treatments are reliable, exact rates of calcification for *P. onkodes* are likely to be understated in experimental conditions compared to the open reef. This is an area that requires further work to determine what is causing this difference in calcification and if it is common to all similar experiments. Flow and wave energy will be important factors that influence the calcification processes and should also be considered in future aquarium designs that seek to test the effects of future acidification scenarios on CCA's.

4.6 What does Mol% Mg-Calcite mean for the CCA physiology and reef processes in a changing climate?

There have been no studies to date which explore the drivers of organism controlled calcification in the key reef-builder *P. onkodes* and what role the Mg content plays in this. Thus it is unclear at this time what influence the mol% $MgCO_3$ has on CCA

physiology and reef processes and even more difficult to anticipate what may happen in the future in a changing climate. Early studies on Mg-C CCA dissolution rates (Plummer and Mackenzie 1974; Bischoff et al., 1987) used CCA that had dolomite and possibly magnesite (see Nash et al., 2013 for discussion) therefore those results were a mix of dissolution rates for 2-3 different magnesium minerals, not just for Mg-calcite with different phases of mol% $MgCO_3$ as was interpreted. Much of our present understanding of biogenic Mg-C dissolution is based on those interpretations (e.g. Andersson et al., 2008). Considering how recent work on CCA dissolution has revealed that a complex suite of interacting mineral, biological, bacterial and chemical factors contribute to net dissolution responses (Nash et al., 2013; Reyes-Nivia et al., 2014; Diaz-Pulido et al., 2014) it has become apparent that the prevailing theory that higher Mg content leads to lower stability is probably not applicable to tropical CCA *P. onkodes*. Indeed there have been no dissolution experiments comparing the dissolution rates of CCA with different mol% $MgCO_3$ to test the correlation of dissolution rates to magnesium content of Mg-C.

.

4.7 Implications for reef management

Finding that dolomite is not affected by ocean acidification in these 3 and 6 month experiments is good news for the survival of CCA species *P. onkodes* under predicted ocean acidification conditions. Dolomite confers stability on the CCA and facilitates its reef-building role (Nash et al., 2013a) as well as being resistant to bacterial bio-erosion (Diaz-Pulido et al., 2014). At this time exact drivers of CCA dolomite formation have not been identified. It seems most likely that dolomite formation is related to provision of a suitable organic substrate, probably being the polysaccharides derived from red algae for agar (Nash et al., 2013a; Zhang et al., 2012). For coral reef management, it is necessary to understand what environmental conditions negatively impact dolomite formation. CCA crust formation is likely to suffer negative affects from reduced recruitment, increased bleaching, bio-erosion and dissolution under higher CO_2 and temperatures (Kuffner et al., 2011; Diaz-Pulido et al., 2012). However, understanding the conditions which negatively impact dolomite formation may enable more effective assessments of the risk that CO_2-driven ocean acidification may pose to important reef-builders such as

P. onkodes. Identifying the drivers and constraints of CCA dolomite formation is an area of research that has not yet been initiated and as such, there is a long way to go to understand what conditions may negatively impact on CCA dolomite formation.

Acknowledgements

Thanks to Frank Brink and the Centre for Advanced Microscopy at the Australian National University for assistance with SEM. Thanks to Florita Flores, Michelle Liddy, Julia Strahl, Paulina Kaniewska and Jordan Hollarsmith for aquarium maintenance and experimental assistance. Funding for the experimental work was provided by the Australian Institute of Marine Science and a Super Science Fellowship from the Australian Research Council. Support for mineral analysis was provided by the Electronic Materials Engineering department at the Research School of Physics, Australian National University.

References

Adey, W. H., Halfar, J., and Williams, B.: The coralline genus Clathromorphum Foslie emend. Adey: Biological, physiological, and ecological factors controlling carbonate production in an Arctic-Subarctic climate archive. Smithsonian contributions to the marine sciences ; number 40, 2013.

Andersson, A. J., Mackenzie, F. T., Bates, N. R.: Life on the margin: implications of ocean acidification on Mg-calcite, high latitude and cold-water marine calcifiers, Mar. Ecol. Prog. Ser, 373, 265-273, 2008.

Anthony, K. R. N., Kline, D. I., Diaz-Pulido, G., Dove, S., Hoegh-Guldberg, O.: Ocean acidification causes bleaching and productivity loss in coral reef builders, PNAS 105, 17442-17446, 2008.

Bischoff, W. D., Mackenzie, F. T., Bishop, F. C.: Stabilities of synthetic magnesian calcites in aqueous solution: Comparison with biogenic materials, Geochim. Cosmochim. Acta. 51, 1413–1423, 1987.

Burdett, H. L., Hennige, S. J., Francis, F. T. Y., and Kamenos, N. A.: The photosynthetic characteristics of red coralline algae, determined using pulse amplitude modulation (PAM) fluorometry, Mar. Biol. Res., 8, 756-763 , 2012.

Caragnano, A. D., Basso, D. E., Jacob, D., Storz, G., Rodondi, F., Benzoni, Dutrieux, E.: The coralline red alga *Lithophyllum kotschyanum* f. *affine* as proxy of climate variability in the Yemen coast, Gulf of Aden (NW Indian Ocean), Geochim Cosmochim Ac
124,1-17, 2014.

Chisholm, J. R. M., Primary productivity of reef-building crustose coralline algae, Limnol. Oceanogr, 48,1376-1387, 2003.

Comeau, S., Edmunds, P. J., Spindel, N. B., Carpenter, R. C.: The responses of eight coral reef calcifiers to increasing partial pressure of CO2 do not exhibit a tipping point, Limnol. Oceanogr, 58, 388-398, 2013.

Darrenougue, N., De Deckker, P., Eggins, S., & Payri, C: Sea-surface temperature reconstruction from trace elements variations of tropical coralline red algae. Quaternary Science Reviews, 93, 34-46, 2014.

Diaz-Pulido, G., Anthony, K., Kline, D. I., Dove, S., Hoegh-Guldberg, O.: Interactions between ocean acidification and warming on the mortality and dissolution of coralline algae, J. Phyc, 48, 32-39, 2012.

617 Diaz-Pulido, G., Nash, M. C., Anthony, K. R. N., Bender, D., Opdyke, B. N., Reyes-
618 Nivia, C., Troitzsch, U.: Greenhouse conditions induce mineralogical changes and
619 dolomite accumulation in coralline algae on tropical reefs, Nat Comms, 5,2014.
620
621 Egilsdottir, H., Noisette, F., Noel, L. M., Olafsson, J., Martin, S.: Effects of pCO2 on
622 physiology and skeletal mineralogy in a tidal pool coralline alga *Corallina*
623 *elongate*, Mar Biol, 160, 2103-2112, 2012.
624
625 Fietzke, J., Ragazzola, F., Halfar, J., Dietze, H., Foster, L. C., Hansteen, T. H.,
626 Eisenhauer, A., and Steneck., R. S.: Century-scale trends and seasonality in pH
627 and temperature for shallow zones of the Bering Sea. P. Natl. Acad. Sci., 112,
628 2960-2965, 2015
629
630 Gaines, A.: Protodolomite redefined, J. Sed. Pet, 47, 543-546, 1977
631
632 Given, R. K., Wilkinson, B. H.: Dolomite abundance and stratigraphic age: constraints on
633 rates and mechanisms of Phanerozoic dolostone formation, J Sediment Petrol 57,
634 1068-1078, 1987.
635
636 Halfar, J., Adey, W. H., Kronz, A., Hetzinger, S., Edinger, E., and Fitzhugh, W. W.:
637 Arctic sea-ice decline archived by multicentury annual-resolution record from
638 crustose coralline algal proxy. P. Natl. Acad. Sci., 110, 19737-19741, 2013.
639
640 Hofmann, L. C., Yildiz, G., Hanelt, D., Bischof, K.: Physiological responses of the
641 calcifying rhodophyte, *Corallina officinalis* (L.), to future CO2 levels, Mar Biol,
642 159, 783-792, 2012.
643
644 Howard, W. R., Nash, M., Anthony, K., Schmutter, K., Bostock, H., Bromhead, D., …
645 Williamson, J.: Ocean acidification. *In* A Marine Climate Change Impacts and
646 Adaptation Report Card for Australia 2012, *Edited by* Poloczanska E, Hobday A,

Richardson A. Centre for Australian Weather and Climate Research, Hobart, TAS,2012.

Jones, B., Luth, R. W., McNeil, A. J.: Powder X-ray diffraction analysis of homogeneous and heterogeneous sedimentary dolostones, J. Sed. Res. 71, 790-799, 2001.

Johnson, M. D., Moriarty, V. W., Carpenter, R. C.: Acclimatization of the Crustose Coralline Alga Porolithon onkodes to variable pCO2, PLoS ONE 9, e87678, 2014.

Kaczmarek, S. E., and Sibley, D. F.: On the evolution of dolomite stoichiometry and cation order during high-temperature synthesis experiments: An alternative model for the geochemical evolution of natural dolomites, Sed. Geol. 240, 30-40, 2011.

Kamenos, N. A., Cusack, M., and Moore, P. G.: Coralline algae are global palaeothermometers with bi-weekly resolution. Geochim. Cosmochim. Acta, 72(3), 771-779, 2008.

Kamenos, N. A., Burdett, H. L., Aloisio, E., Findlay, H. S., Martin, S., Longbone, C., Dunn, J., Widdicombe, S., and Calosi, P.: Coralline algal structure is more sensitive to rate, rather than the magnitude, of ocean acidification, Global Change Biology, 19, 3621-3628, 2013.

Kuffner, I. B., Andersson, A. J., Jokiel, P. L., Rodgers, K. S., Mackenzie, F. T.: Decreased abundance of crustose coralline algae due to ocean acidification, Nat Geoscience, 1, 114-117, 2007.

Morse, J. W., Arvidson, R. S., Lüttge, A.: Calcium carbonate formation and dissolution, Chem Rev, 107, 342-381, 2007.

Nash, M. C., Troitzsch, U., Opdyke, B. N., Trafford, J. M., Russell, B. D., Kline, D. I.:First discovery of dolomite and magnesite in living coralline algae and its geobiological implications, Biogeosciences, 8, 3331-3340, 2011.

Nash, M. C., Opdyke, B. N., Troitzsch, U., Russell, B. D., Adey, W. H., Kato, A., ... Kline, D. I., Dolomite-rich coralline algae in reefs resist dissolution in acidified conditions, Nat Climate Change, 3, 268-272, 2013a.

Nash, M. C., Opdyke, B. N., Wu, Z., Xu, H., Trafford, J. M.: Simple x-ray diffraction techniques to identify mg-calcite, dolomite, and magnesite in tropical coralline algae and assess peak asymmetry, J Sediment Res 83, 1085-1099, 2013b.

Pueschel, C. M., Judson, B. L., and Wegeberg, S. : Decalcification during epithallial cell turnover in Jania adhaerens (Corallinales, Rhodophyta).Phycologia, 44,156-162, 2005.

Ramirez-Reinat, E. L., and Garcia-Pichel, F.: Characterization of a marine cyanobacterium that bores into carbonates and the redescription of the genus Mastigocoleus, J. Phycol. 48, 740-749, 2012.

Ries, J. B.: Skeletal mineralogy in a high CO2 world, J. Exp. Mar. Biol. Ecol. 403, 54-64, 2011.

Mackenzie, F. T., Arvidson, R. S., Guidry, M. W.: Chemostatic models of the ocean atmosphere-sediment system through Phanerozoic time, Mineral Mag. 72, 329-332, 2008.

Orr, J.: Recent and future changes in ocean carbonate chemistry, in Ocean Acidification (eds Gattuso JP, Hansson L) Chpt 3, 41-66, 2011.

Plummer, L. N., Mackenzie, F. T.: Predicting mineral solubility from rate data: Application to the dissolution of magnesian calcites, Am. J. Sci. 274, 61–83, 1974.

Ragazzola, F., Foster, L. C., Form, A., Anderson, P. S., Hansteen, T. H., Fietzke, J.: Ocean acidification weakens the structural integrity of coralline algae, Glob Change Biol, 18, 2804-2812, 2012.

Ragazzola, F., Foster, L. C., Form, A. U., Buscher, J., Hansteen, T. H., Fietzke, J.: Phenotypic plasticity of coralline algae in a high CO_2 world, Ecol Evol 3, 3436-3446, 2013.

Reyes-Nivia, C., Diaz-Pulido, G., Dove, S.: Relative roles of endolithic algae and carbonate chemistry variability in the skeletal dissolution of crustose coralline algae, Biogeosciences Discussions 11, 2993-3021, 2014.

Saller, A. H.: Petrologic and geochemical constraints on the origin of subsurface dolomite, Enewetak Atoll: An example of dolomitization by normal seawater, Geology, 12, 217-220. 1984.

Smith, A. M., Sutherland, J. E., Kregting, L., Farr, T. J., Winter, D. J.: Phylomineralogy of the Coralline red algae: Correlation of skeletal mineralogy with molecular phylogeny, Phytochemistry, 81, 97-108, 2012.

Steneck, R. S.: The ecology of coralline algal crusts: convergent patterns and adaptative strategies. Annual Review of Ecology and Systematics, 273-303, 1986.

Tucker, M. E.: Precambrian dolomites: petrographic and isotopic evidence that they differ from Phanerozoic dolomites, Geology, 10, 7-12, 1982.

737 Uthicke, S., Pecorino, D., Albright, R., Negri, A. P., Cantin, N., Liddy, M., Dworjanyn,
738 S., Kamya, P., Byrne, M., Lamare, M.: Impacts of Ocean Acidification on Early
739 Life-History Stages and Settlement of the Coral-Eating Sea Star *Acanthaster*
740 *planci*, PLoS ONE 8, e82938, 2013.
741
742 Vasconcelos, C., McKenzie, J. A.: Microbial mediation of modern dolomite precipitation
743 and diagenesis under anoxic conditions (Lagoa Vermelha, Rio de Janeiro, Brazil),
744 J Sediment Res, 67, 378-390, 1997.
745
746 Wilkinson, B. H., Given, R. K.: Secular variation in abiotic marine carbonates:
747 Constraints on Phanerozoic atmospheric carbon dioxide contents and oceanic
748 Mg/Ca ratios, J. Geol, 94, 321-333, 1986.
749
750 Zhang, F., Xu, H., Konishi, H., Shelobolina, E. S., Roden, E. E.: Polysaccharide-
751 catalyzed nucleation and growth of disordered dolomite: A potential precursor of
752 sedimentary dolomite, Am Mineral, 97, 556-567, 2012.
753
754 Zhang, F., Xu, H., Shelobolina, E. S., Konishi, H., Converse, B., Shen, Z., and Roden, E.
755 E.: The catalytic effect of bound extracellular polymeric substances excreted by
756 anaerobic microorganisms on Ca-Mg carbonate precipitation: Implications for the
757 “dolomite problem”. Am. Mineral.,100, 483-494, 2015.
758
759 Zhao, H., and Jones, B.: Origin of “Island dolostones”: a case study from the Cayman
760 Formation (Miocene), Cayman Brac, British West Indies, Sed. Geol. 243-244,
761 191-206, 2012.
762
763
764 **Figure Legends**
765 **Table 1:** Two factor analysis of variance (ANOVA) testing for difference in mol%
766 $MgCO_3$ and Asymmetry indicating dolomite, between different CO_2 treatments (Factor
767 Treatment) and experimental growth versus pre-experimental growth (Factor Type). No

768 significant difference related to CO_2 treatments, but significant difference between
769 experimental and pre-experimental growth for both mol% $MgCO_3$ and dolomite
770 asymmetry.

771 **Figure 1:** Example of *Porolithon onkodes* (CCA) after 3 months. New pigmented crust
772 overgrowing resin used for XRD.

773 **Figure 2:** Magnesium composition for experimental growth of *P. onkodes*. Mol% is for
774 Mg-calcite mol% $MgCO_3$. Asymm mol% includes influence of dolomite asymmetry on
775 calculated Mg-calcite mol% $MgCO_3$, the more dolomite present the higher the Asymm
776 mol%. **(a)** New crust after 3 months. **(b)** New crust after 6 months. There was no
777 significant difference between treatments for either the mol% $MgCO_3$ or the Asymm
778 mol% in new crust after 3 or 6 months. 778 control samples were unavailable for
779 mineral analyses. **(c)** New settlement after 6 months. As for the new crust, there was no
780 significant difference across the treatments in mol % $MgCO_3$. There is no dolomite in the
781 new settlement consistent with the absence of white crust. Error bars are ± 1 s.d.

782 **Figure 3:** Magnesium composition for CCA new settlement, 3 month crust, 6 month
783 crust, and pre-experimental crust. The mol% $MgCO_3$ in the Mg-calcite increases from
784 new settlement to 3 and 6 months, and again for the pre-experimental crust. Dolomite is
785 not present in the new settlement, appears within 3 months, increases in amount in the 6
786 month new crust, but is highest in the pre-experimental crust. Error bars are 1 s.d.

787 **Figure 4:** SEM (Backscatter -BSE) of control *P. onkodes* showing dolomite in
788 experimental and pre-experimental growth. BSE SEM shows the lighter elements i.e.
789 magnesium, as darker gray and heavier elements, i.e. calcium are pale gray to white.
790 Secondary electron images show the topography of the sample but do not provide
791 information on the elemental composition. EDS measurements are made in the different
792 gray shade areas to measure Mg composition (range listed in supplement) and this is used
793 to identify the mineral composition. Once the measurements have been made it is
794 possible then to identify dolomite and calcite from the gray shade. **(a)** Experimental
795 growth- dolomite (D) Dolomite-composition material in cell. This is not the typical cell
796 lining but has been observed in other CCA. Mg-calcite (Mg-C). Scale = 2 microns. **(b)**

797 Experimental growth: micro-scale lumpy dolomite lining cell. Scale = 1 micron. Cell
798 growth in experimental growth is less regular and organized than pre-experimental
799 growth. **(c)** Dolomite cell lining in pre-experimental growth. Notice the very narrow cell
800 walls. **(d)** Dolomite infill in a reproductive conceptacle in the old growth. Cells below
801 conceptacle are all in-filled with dolomite. Scale bars: a and c = 2 microns, b = 1 micron,
802 d = 10 microns.

803 **Figure 5:** Control *P. onkodes* with experimental growth on pre-experimental growth. **(a)**
804 (BSE) There is a visible difference in the appearance of experimental crust (black arrow)
805 to the pre-experimental growth (black dashed arrow). The lighter grey of the surface is
806 due to less magnesium (dolomite) infilling the cells that appear as darker grey infill in the
807 pre-experimental lower part of the crust. Black box enlarged in **b**. D is dolomitised
808 conceptacle. **(b)** Close up showing the consistent presence of infill in pre-experimental
809 growth whereas in the new growth regular dolomite cell lining is absent. Also, the Mg-C
810 crust itself appears to be less dense with many cracks from the cutting visible in the new
811 growth but not so in the pre-experimental growth. **(c)** Secondary electron image of
812 control CCA. The pre-experimental growth appears to have a fine opaque organic film
813 covering part of the cut crust (white dashed arrow), but this is not present in the
814 experimental growth (White arrow). **(d)** Control CCA (BSE) Dashed arrow to pre-
815 experimental growth. Grey cells are dolomite infill. Black arrow to experimental growth,
816 generally an absence of dolomite infill, note line of porosity in transition between pre-
817 experimental and experimental growth. Scale bars: a, c and d = 100 microns, b = 20
818 microns.

819 **Figure 6**:Transition from pre-experimental crust to experimental crust in *P. onkodes*, pre-
820 industral CCA **(a, b) (BSE)**, high CO_2 CCA **(c, d)**. Transition from pre-experimental
821 growth to experimental identified by following the growth lines from the crust on the
822 resin (not pictured) across the sample. **(a)** overview, brackets- new growth. **(b)** close up
823 of transition. Crust below dashed line is pre-experimental growth. Dolomite infills cells
824 (black arrows). Above dashed line new growth does not have cells infilled, crust has
825 been damaged by saw cut. **(c)** Overview of transition to new growth in high CO_2 CCA,
826 brackets – new growth. **(d)** close up of transition. Similarly to control and pre-industrial

CCA, cells in pre-experimental growth are infilled with dolomite (black arrows). Crust above dashed line grew during experiment. Cells are not infilled with dolomite and crust has crushed under the sawcut. Scale bars a, b, c and d = 20 microns. Close up of transition between from pre-experimental growth to experimental growth in supplement Fig. 3.

Figure 7: SEM (BSE) of Control *P. onkodes* (AC4). **(a)** Overview of experimental growth, pre-experimental growth and transition zone (bracket). Cells at the surface do not have dolomite. White box enlarged in B. **(b)** Cells in experimental growth have no dolomite infill. Cells below experimental growth have dolomite lining the cells but the centres are in-filled with aragonite. White box enlarged in C, black box enlarged in E. **(c)** close up of cell infill by aragonite within the dolomite lining. **(d)** Dolomite lined cell in transition zone with aragonite infill. **(e)** Patch of crust below experimental growth with aragonite infill. **(f)** Close up of dolomite-lined cell with aragonite infill. Scale bars: a and b = 20 microns, c and f = 1 micron, d = 2 microns, e = 10 microns.

Figure 8: SEM (BSE) of varied mineral fabrics in CCA. **(a)** Alteration of base of CCA crust by bacteria to aragonite (Diaz-Pulido et al., 2014), remnant CCA cells are visible in the aragonite (A) confirming it was CCA crust and not coral substrate. **(b)** Hypothallus cells grow parallel to substrate then grow vertically and are in-filled with dolomite (D). In-fill of micro-borer trace by aragonite and dolomite rim (arrow). **(c)** Band of dolomite between aragonite alteration and undamaged cells. (**d**) Damaged crust has been in-filled with new cell growth rich in dolomite. Scale bars: a = 100 microns, b, c and d = 20 microns.

	Mol %				Asymmetry			
	DF	MS	F	p	DF	MS	F	p
Treatment	2	1.76E-05	0.77	0.4754	2	1.98E-04	0.55	0.582
Type	1	6.52E-04	28.54	**< 0.001**	1	7.00E-03	19.57	**<0.001**
Tr X Type	2	0.49	0.61972	0.1195	2	0.35	0.7082	0.099

Residual	21		22	3.58E-04

851

852 Table 1

853

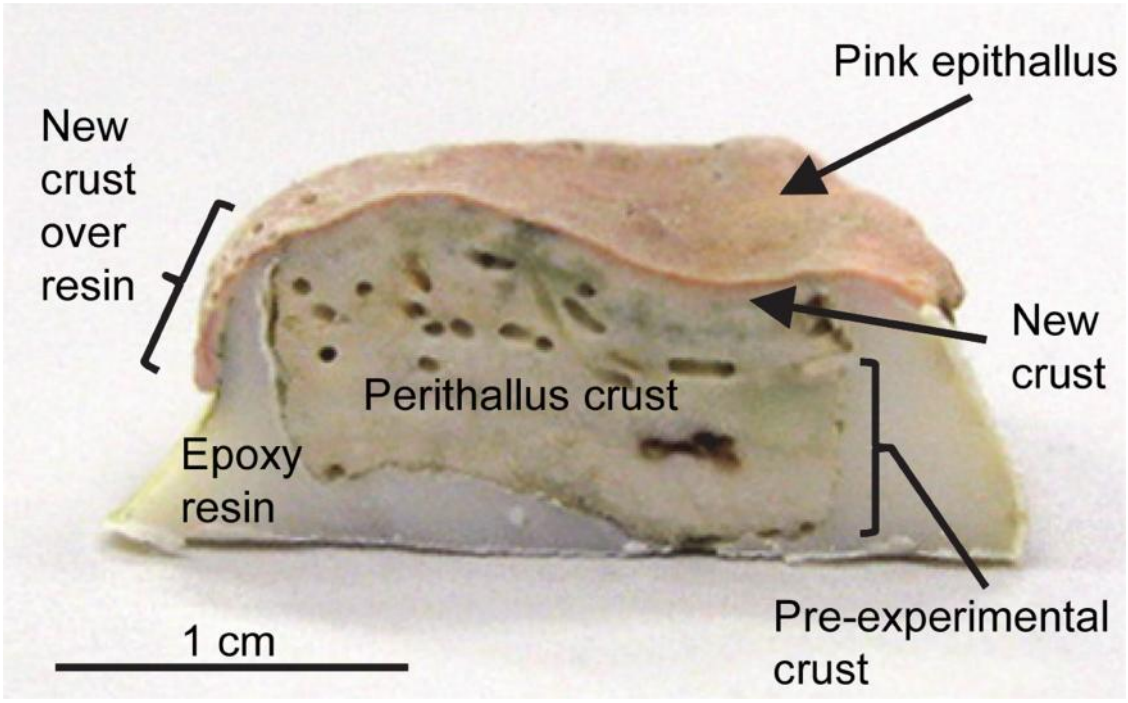

854

855 Figure 1

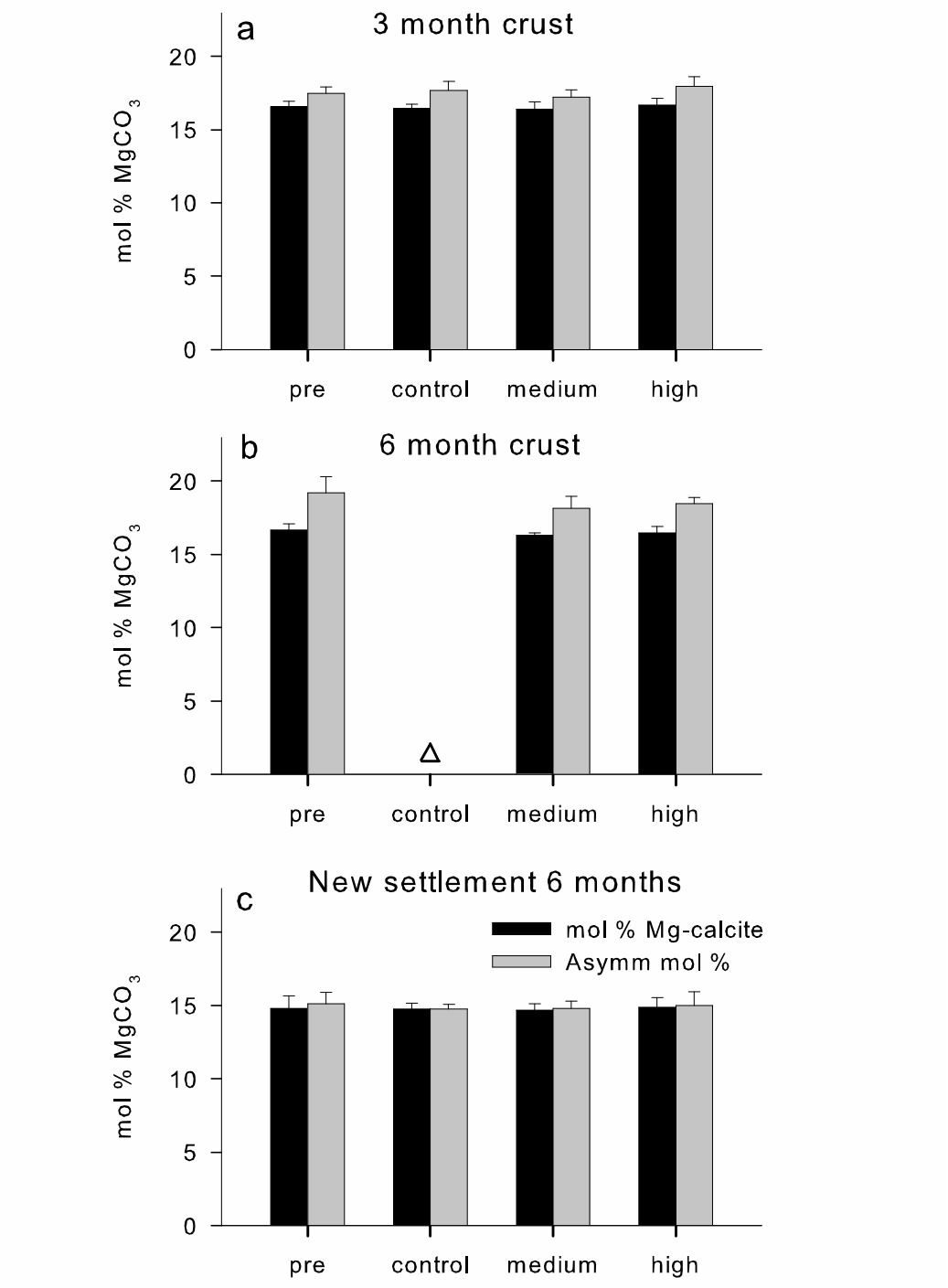

856

857 **Figure 2**

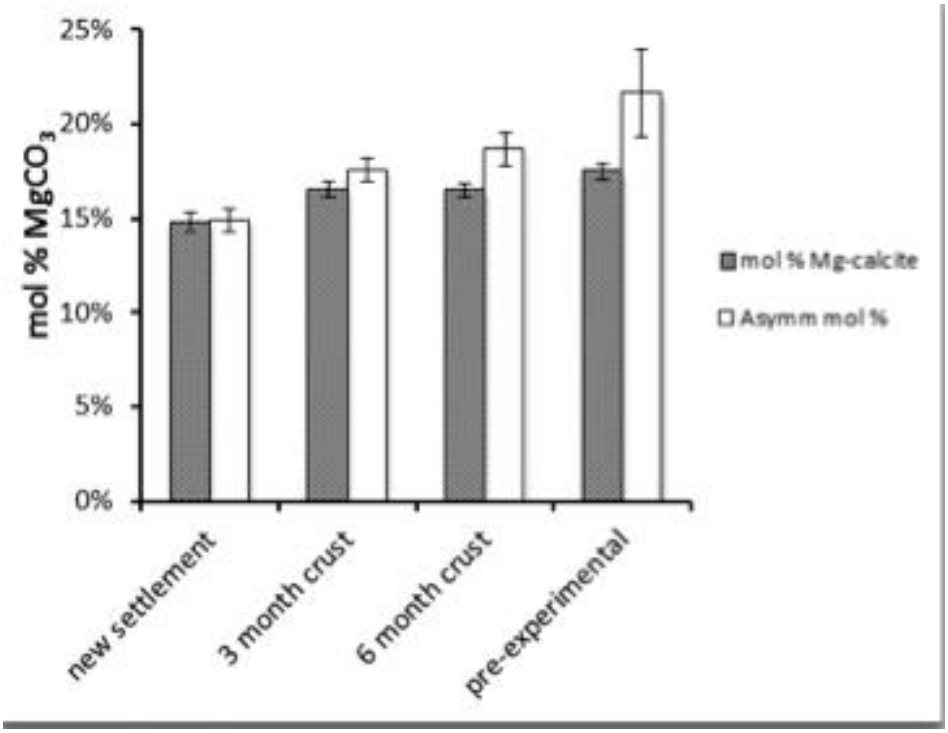

858

859 **Figure 3**

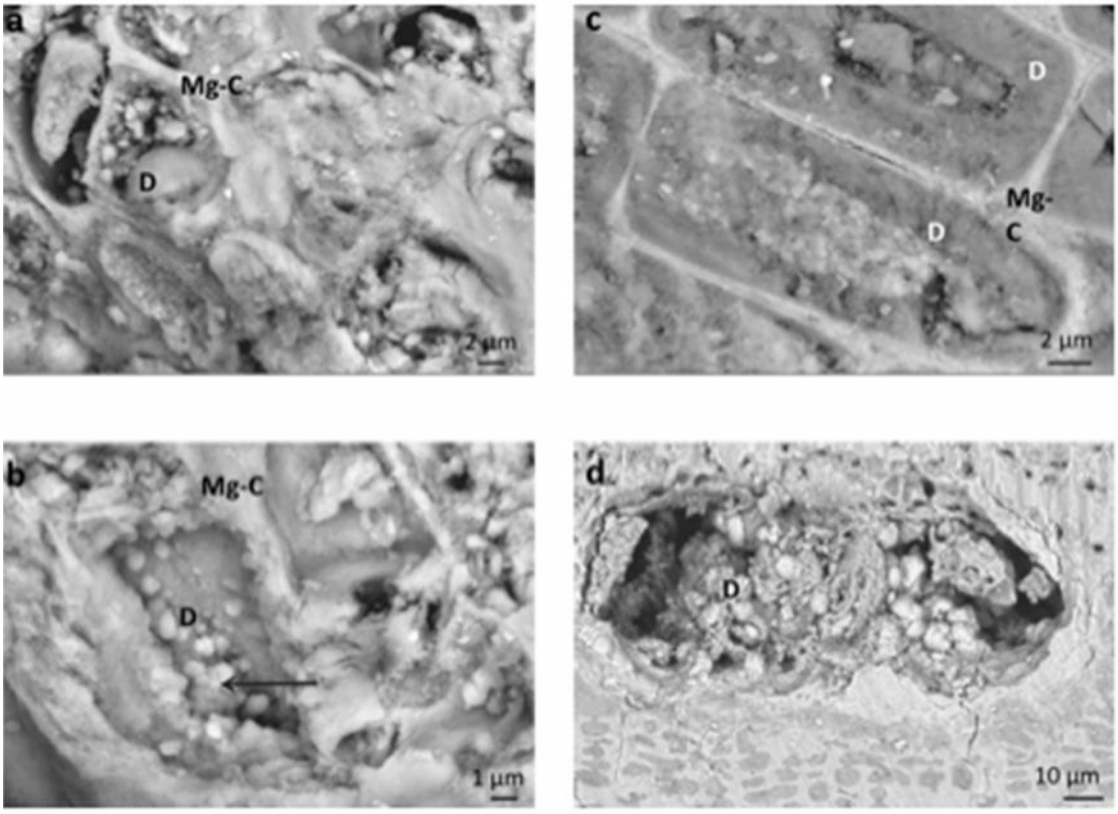

860

861 **Figure 4**

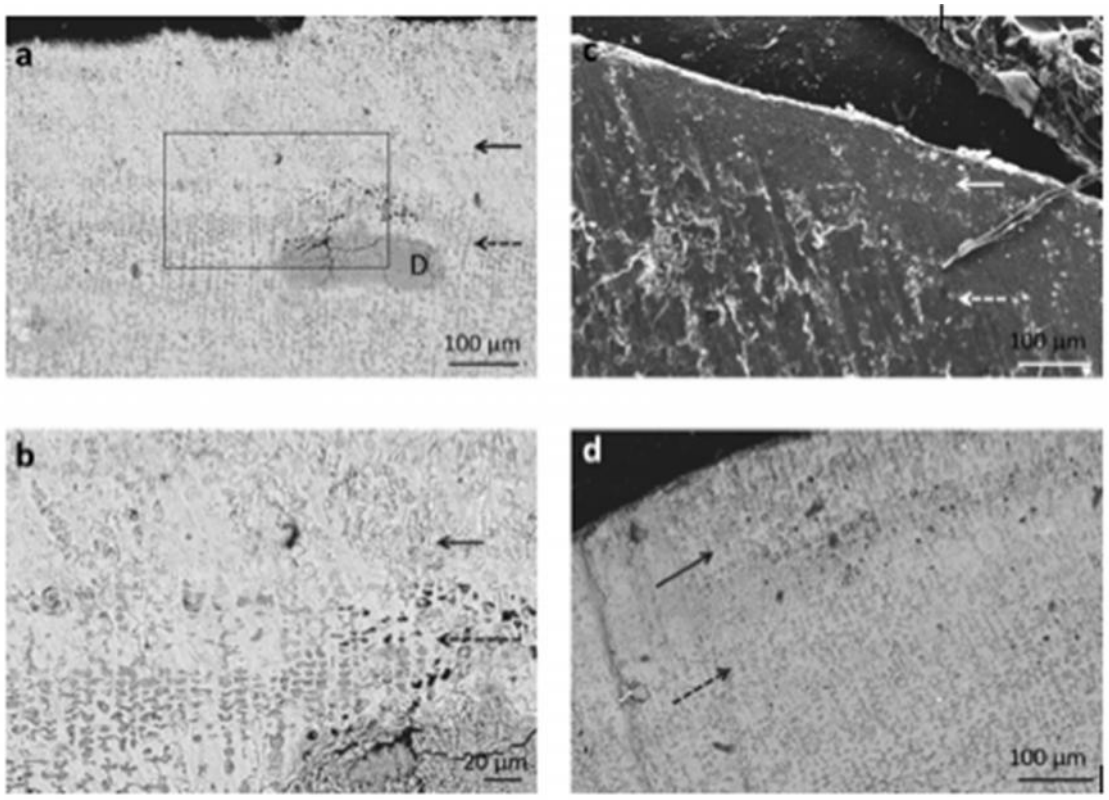

Figure 5

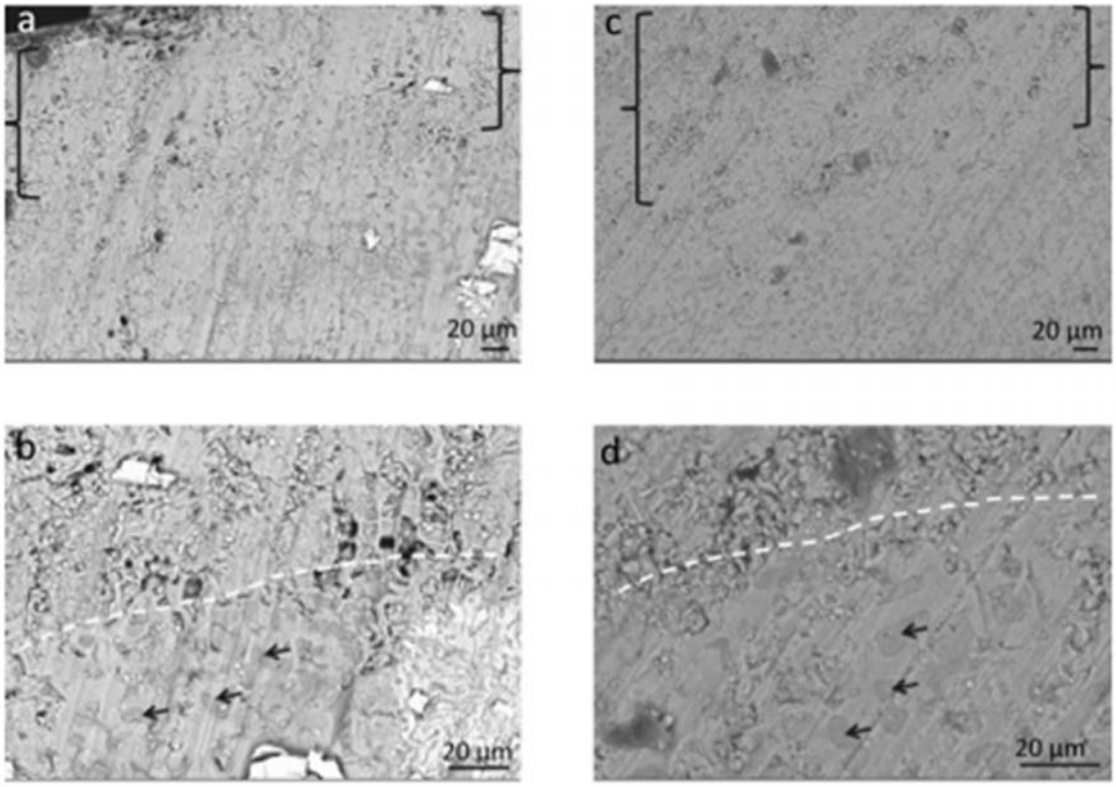

865 **Figure 6**

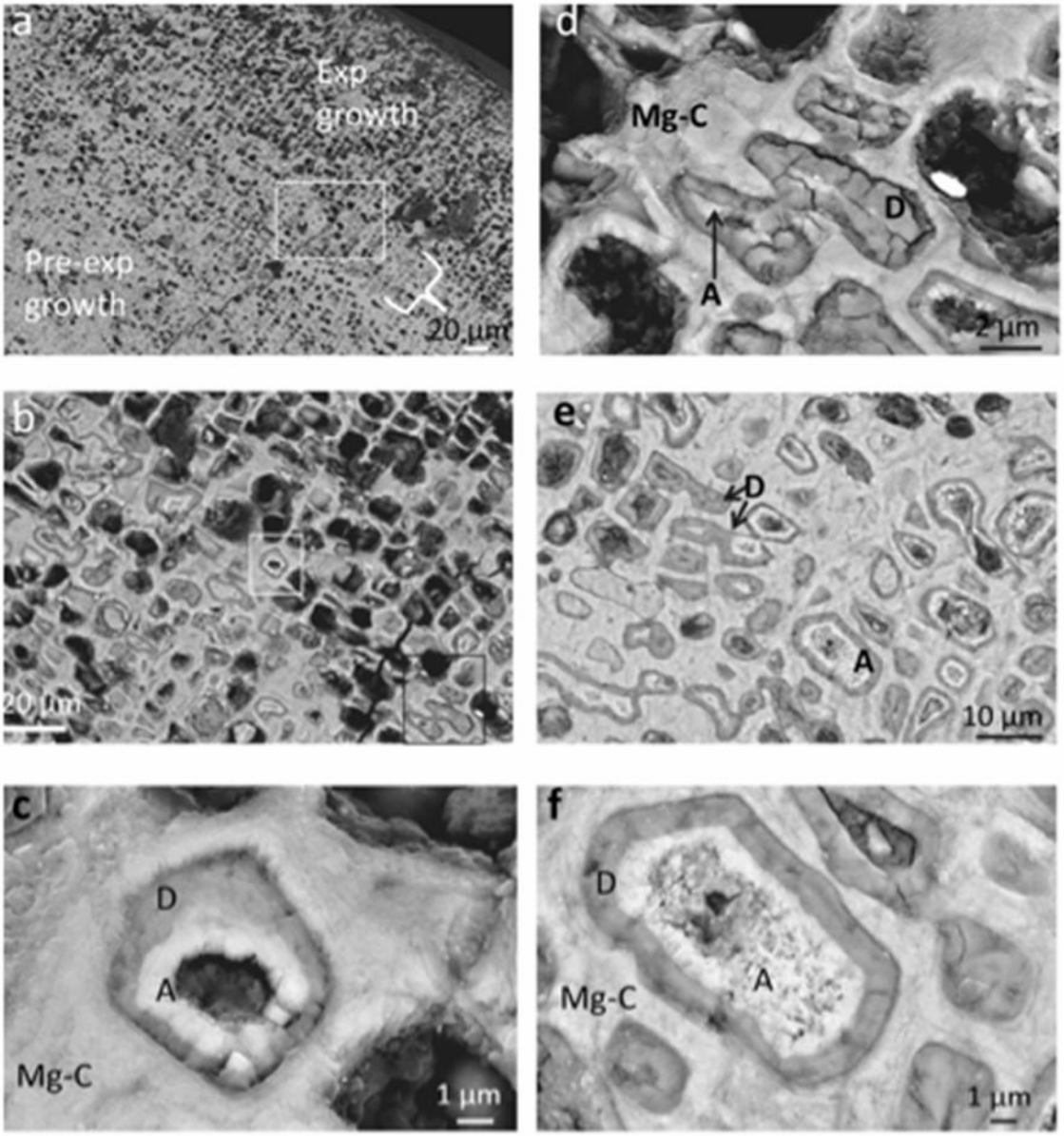

866

867 **Figure 7**

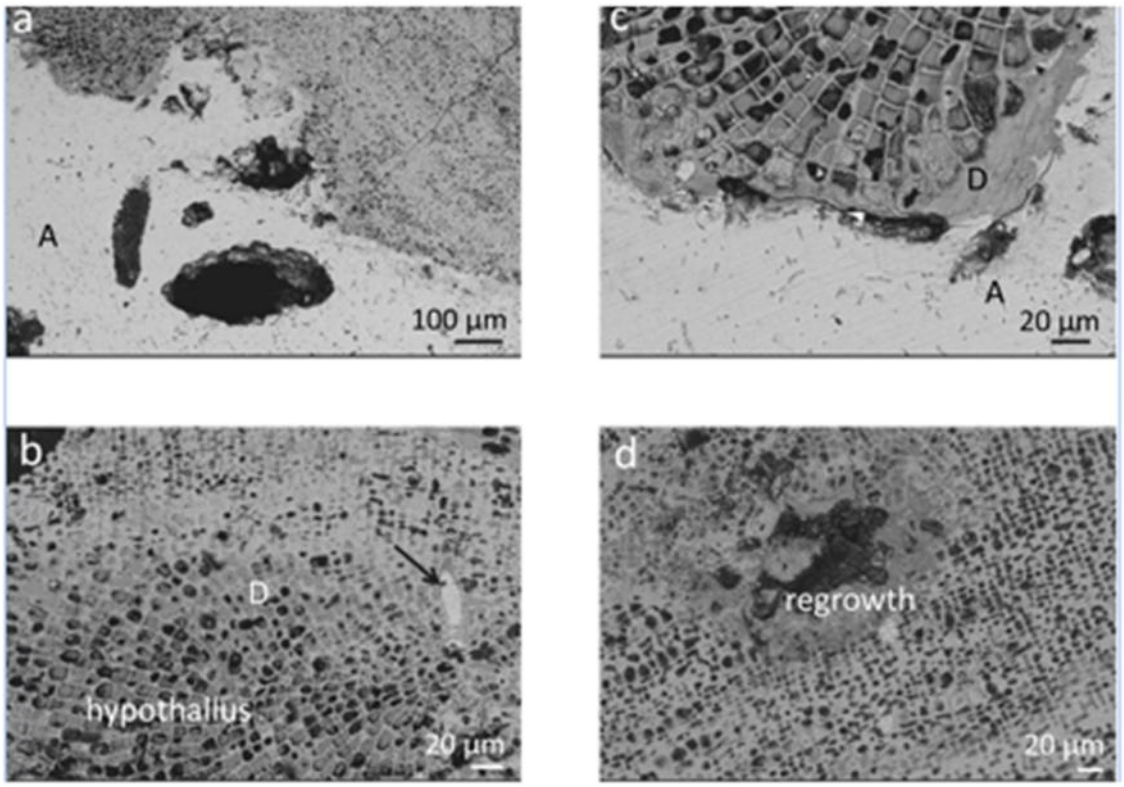

Figure 8